Pitch-based ribbon-shaped carbon-fiber-reinforced one-dimensional carbon/carbon composites with ultrahigh thermal conductivity

Guanming Yuan [a], Xuanke Li [a]*, Zhijun Dong [a], Xiaoqing Xiong [a], Brian Rand [b], Zhengwei Cui [a], Ye Cong [a], Jiang Zhang [a], Yanjun Li [a], Zhongwei Zhang [c], Junshan Wang [c]

a Hubei Province Key Laboratory of Coal Conversion & New Carbon Materials, Wuhan University of Science and Technology, Wuhan 430081, China;

b SARChI Chair of Carbon Technology and Materials, Institute of Applied Materials, University of Pretoria, Pretoria 0002, South Africa;

c Aerospace Research Institute of Materials and Processing Technology, Beijing, 100076, China.

Abstract: Ribbon-shaped carbon fibers have been prepared from mesophase pitch by melt-spinning, oxidative stabilization and further heat treatment. The internal graphitic layers of ribbon-shaped carbon fibers graphitized at 2800 °C show a highly preferred orientation along the longitudinal direction. Parallel stretched and unidirectional arranged ribbon-shaped carbon fibers treated at about 450 °C were sprayed with a mesophase pitch powder grout, and then hot-pressed at 500 °C and subsequently carbonized and graphitized at various temperatures to produce one-dimensional carbon/carbon (C/C) composite blocks. The shape and microstructural orientation of ribbon fibers have been maintained in the process of hot-pressing and subsequent heat treatments and the main planes of the ribbon fibers are orderly accumulated along the hot-pressing direction. Microstructural analyses

* Corresponding author. Tel.: Fax: +0086 27 86556906
E-mail address: xkli8524@sina.com (X. Li)

indicate that the C/C composite blocks have a typical structural anisotropy derived from the unidirectional arrangement of the highly oriented wide ribbon-shaped fibers in the composite block. The thermal conductivities of the C/C composites along the longitudinal direction of ribbon fibers increase with heat-treatment temperatures. The longitudinal thermal conductivity and thermal diffusivity at room temperature of the C/C composite blocks graphitized at 3100 °C are 896 W/m K and 642 mm^2/s, respectively.

1. Introduction

Carbon/carbon (C/C) composites are extensively used as the friction material in aircraft brakes, nose-cones of ballistic missiles, leading edges in high-performance aerospace vehicles such as the US Space Shuttle, and as turbine rotors and other high-temperature engine and rocket components [1,2]. Recently, the range of applications has been broadened to include thermal management (heat sinks) in electronic components and heat pipes where the C/C composites with very high thermal conductivity are advantageous [3,4]. During last few decades there has been great interest in the development of C/C composites with unique thermophysical properties for high performance thermal management systems including heat sinks, electronic packaging and plasma facing components of fusion devices [4]. These strategic applications need the candidate materials to have high thermal conductivity, low coefficient of thermal expansion and good mechanical strength. For instance, crystalline graphite is a promising material for heat sinks, which can offer a thermal conductivity of around 2800 W/m K at 300 K parallel to the in-plane direction, 7 times that of copper, but crucially, this property is highly anisotropic and decreases dramatically as the angular direction with respect to the layer planes increases.

Therefore, it is required to precisely control the microstructural features of bulk C/C composite materials, which also possess a wide variety of directional properties depending upon which microstructures predominate with varying degrees of preferred orientation and perfection in the graphitic crystallites.

It is well known that the thermal conductivity of C/C composites is structure sensitive (directional dependent). The composite architecture, the thermal conductive property, volume fractions, texture and crystallinity of carbon fibers themselves, as well as the spatial arrangement of voids and other defects in C/C composites, have obvious influence on their thermal conductivity. Among the above-mentioned factors, the physical properties of carbon fibers can vary over a wide range depending on the organic precursor and processing conditions used. Mesophase pitch-based graphite fibers are known to have greater thermal and electrical conductivity and higher Young's modulus than those derived from polyacrylonitrile [5,6], so that they have found applications as thermal management materials [7-9] due to their excellent thermal transport properties. The most thermally conductive, commercially available mesophase pitch-based graphite fiber, Thornel K-1100, has a nominal thermal conductivity value of 1000 W/m K, which is a direct result of the highly crystalline graphitic structure and its high degree of orientation parallel to the fiber axis [6]. Therefore, great research efforts are concentrated on the development of high thermal conductivity C/C composites made with mesophase pitch-based high modulus carbon fibers, which are generally acting as thermal conductive reinforcements [4,7,10,11]. Recently, Ma et al. [12,13] have reported the self-adhesion preparation of unidirectional C/C composites from the appropriately oxidized ribbon-shaped carbon fibers. These composites, with a high thermal conductivity of 837 W/m K in the longitudinal direction of fibers, were obtained through firstly hot-pressing at 2400 °C

with a pressure of 30 MPa, and finally graphitization at 3000 °C. However, the precise control of thermosetting or appropriate oxidation degree to the pitch fibers in order to maintain good moldability (i.e., incomplete stabilization and fixing the adhesive/ bonding components in the fibers) and crystal orientation, is very complicated in the preparation process. In addition, simplification of the fabrication process is also necessary to decrease the cost of C/C composites.

Previous work at Clemson University has shown that the crystal orientation in mesophase pitch-based fibers with ribbon shape is more aligned, parallel to the fiber axis, than that of traditional commercial round-shaped fibers, and the corresponding thermal conductivity of ribbon fibers graphitized at only 2400 °C can be comparable with that of commercial round-shaped fiber graphitized at above 3000 °C [14-16]. In comparison with the conventional round-shaped carbon fibers, the ribbon-shaped fibers possess excellent thermal transport property and much larger cross-sectional area [17-19], which allows the high volume fraction stacking of this highly crystal oriented flat fibers in a unidirectional laminate to form the C/C composites with high bulk density and excellent thermophysical property.

In this work, the preparation and characterization of highly oriented C/C composite blocks using the 450 °C treated ribbon fibers as a matrix material and mesophase pitch powder grout as a binder are reported. The influence of heat treatment temperatures (HTTs) on the bulk densities and the electrical, as well as thermal conductive properties, of the resultant C/C composites is investigated. The relationships between the thermal conductivity and the electrical resistivity as well as microcrystalline parameters of the C/C composites are also discussed.

2. Experimental

2.1. Raw materials

A commercial naphthalene-derived synthetic mesophase pitch produced by Mitsubishi Gas Chemical Corporation was directly used as a raw material to produce the pitch fibers by melt spinning. This type of mesophase pitch has 100% anisotropic content, a softening point of 265 °C and a high carbon yield of about 80% determined at 900 °C for 3 h. The mesophase pitch powder, obtained by milling in a hammer-mill crusher and then sieving through a 200 mesh screen, was also used as a binder for the C/C composite molding.

2.2. Preparation and pre-treatment of ribbon-shaped pitch fibers

Uniformly molten mesophase pitch in a heating tank was extruded under pressurized nitrogen of ~0.2 MPa, through a slit shaped die with an aspect ratio of about 80, at a spinning temperature of 320~330 °C, and the extrudate was then drawn through a winding drum at a certain rotational speed controlled by a servo motor to form ribbon-shaped pitch fibers.

The as-spun pitch fibers with ribbon shape were stabilized at 240~250 °C in an O_2 atmosphere for 10~20 h at a flowing rate of ~200 ml/min. The stabilized fibers have a slightly higher carbon yield of about 84%, in comparison to that of mesophase pitch. The obtained stabilized fibers were subsequently heat treated to about 450 °C for 1 h under a N_2 atmosphere in order to slightly increase their mechanical strength in the process of C/C composite molding. That is to say that the usefulness of this 450 °C pre-heat treatment is for strengthening the stabilized fibers to prevent them subsequently breaking due to shrinkage during hot pressing. Such pretreated ribbon fibers and mesophase pitch fine powder were used as a starting filler and the binder (namely matrix) to prepare one-dimensional C/C composites.

2.3. Preparation of one-dimensional C/C composites

The ribbon-shaped fibers heat-treated at about 450 ℃ were sprayed by a uniformly mixed solution composed of mesophase pitch fine powder and isopropyl alcohol at a volume ratio of 1:8. The air-dried ribbon fibers coated with pitch powder were uniaxially and evenly arranged in a stainless steel mould and then hot-pressed at 500 ℃ for 5 h under a pressure of 10 MPa to produce a unidirectional C/C composite block with dimensions of 100 × 90 × 20 mm. The as-prepared C/C composite blocks were finally carbonized and graphitized at various temperatures. Carbonization treatment to ~1000 °C was usually carried out slowly (10 °C/h) in order to inhibit the rapid release of volatiles, and to prevent or decrease the delaminating or cracking of the unidirectional laminates. The carbonized C/C composite blocks were loaded in a graphite crucible and placed in the furnace. The furnace was vacuum purged and then argon gas was introduced to form a pressure of 0.1 MPa. The furnace was heated to various graphitization temperatures and dwelled for 15 min, as required.

2.4. Characterization of the unidirectional C/C composites

The specimens were mechanically cut from the as-prepared, carbonized and graphitized C/C composite blocks, polished and ultrasonically washed in ethyl alcohol for 0.5 h. The preferred orientation structure of the resultant blocks was determined by X-ray diffraction (XRD) analysis using a Cu Kα radiation (λ = 0.15406 nm). Microstructure, morphology and texture of the C/C composites were imaged with a NOVA 400 NANO field emission scanning electron microscopy (SEM) and a Carl Zeiss AX10 polarized light microscopy (PLM) in reflectance mode.

The bulk density (ρ) of the sample with a rectangular-shaped block was calculated from its mass and dimensions. The electrical resistivity of each sample was measured by the standard four-probe method on a TTi BS 407 precision milli/micro ohmmeter.

The thermal diffusivity (α) of the specimen with size of 10 × 10 × 4 mm was measured using a laser-flash diffusivity instrument (LFA 457, NETZSCH) at room temperature. The values of specific heat (C_p) determined using a differential scanning calorimeter (STA 449C, NETZSCH) ranged between 50~1300 °C from 0.78 to 2.2 J/g K. The room-temperature C_p value of the samples was about 0.75 J/g K, which is among the values (0.72~0.99 J/g K) reported in references [4,20,21]. The thermal conductivity (λ) of the samples was then calculated from the bulk density, specific heat capacity and thermal diffusivity according to the equation: $\lambda = \rho \cdot C_p \cdot \alpha$. Each sample was tested in at least three sections and the average thermal diffusivity of the three measurements was calculated. Both the electrical resistivity and thermal conductivity data were obtained along the longitudinal direction of ribbon fibers. The bending strengths of the C/C composites were measured perpendicular to the longitudinal direction of ribbon fibers at room temperature on a CMT 4303 computer-controlled mechanical testing machine.

3. Results and discussion

3.1. Morphology and structure of ribbon-shaped carbon fiber

Fig. 1(a) shows the typical SEM image of a whole ribbon-shaped carbon fiber after oxidative stabilization, low temperature heat treatment and finally high temperature graphitization at 2800 °C. It can be seen from Fig. 1(a) that the obtained fiber possesses a relatively uniform ribbon shape and smooth lamellar orientation parallel to the flat plane of the ribbon and without any deformation or cracking during the entire treatment process (stabilization, carbonization and graphitization), as reported in reference [22], which is distinct from the open wedge crack texture of some round-shaped carbon fibers derived from mesophase pitch, with a radial texture on the

transverse section [23,24]. The average width and average thickness of ribbon-shaped carbon fiber were ~1.1 mm and ~15 μm, which undergo a marked bulk shrinkage of about 45% from the as-spun pitch fiber (~1.5 mm and ~20 μm). The cross-sectional area of ribbon fiber was ~350 times more than that of conventional round-shaped carbon fibers with a diameter of ~8 μm. The ribbon-shaped fiber appears to show continuous structural integrity. The graphite crystals at the center (main plane) and edge sections of the ribbon-shaped fiber shown in Fig. 1(b-d), show clear variations in orientation. The SEM image from the center of the ribbon-shaped fiber in Fig. 1(b) shows a strong preferred orientation along the longitudinal direction and parallel to the main surface of the ribbon fibers. Partial radial or wrinkled texture can be seen from Fig. 1 (c and d), showing that the carbon layers at the two edges of the ribbon exhibit a preferred orientation along the longitudinal direction of the ribbon fiber and around the edge outline. The carbon layers at the center of the ribbon fiber display more perfect orientation than that of two edge sections. This texture is opposite to that observed by Edie and co-workers [14,15] in their ribbon-shaped fibers of much lower aspect ratio and is the same as that reported for similar ribbon-shaped fibers by Lu et al [17]. The highly preferred oriented crystal structure of the ribbon fiber may have obvious advantage to improve the thermal conductivity of carbon fiber and its C/C composite. No crack from the edge to the center of the ribbon-fiber, especially at the interfaces or connections of different crystal orientations, was observed. The thickness change of the ribbon fiber changes from about 10 μm at the center to about 18 μm at the edge as can be observed from Fig. 1(a-d), which is similar to the morphology of the mesophase pitch-based carbon tape with a thickness in the range of 10~30 μm reported by Shinohara's group [25]. In comparison with the 450 °C heat-treated ribbon fibers with a uniform thickness of about 20 μm, the obvious thickness difference at

the center and the edge of the ribbon fibers, after heat-treatment at 2800 °C, may have a close relation with the different crystal orientations at the two areas of the ribbon fibers. Fig. 1(e) shows a suggested structural diagram (without consideration of the virtual differentia of thickness) of the graphitized ribbon-shaped fiber. The different crystal orientations at the center and the edge of the ribbon-shaped fiber may lead to the anisotropy of the structure and thermal conduction property of the resultant C/C composites.

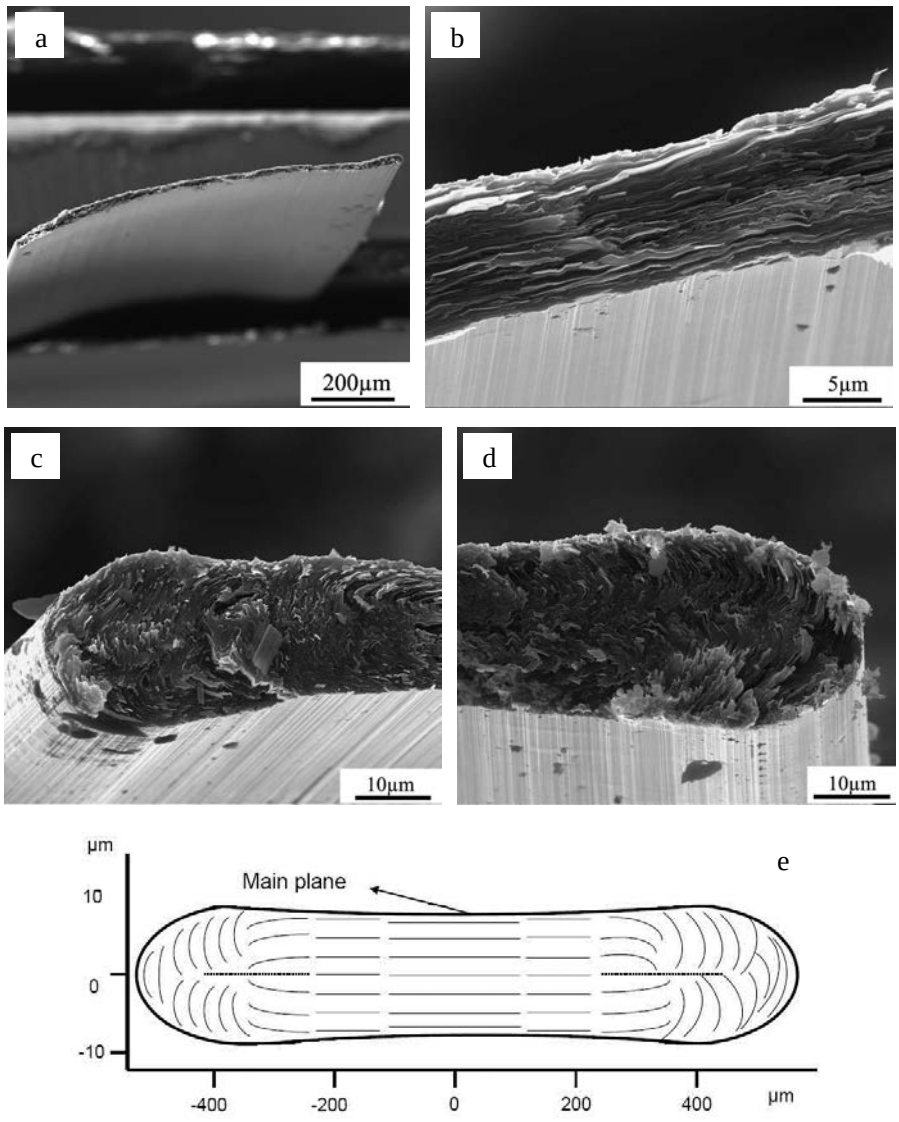

Fig. 1 SEM images of (a) a whole ribbon-shaped carbon fiber after graphitization at 2800 °C and its magnified transverse section at (b) center and (c) left edge and (d)

right edge. A structural diagram (e) of the carbon layer orientation at the transverse section of the ribbon-shaped fiber is also shown.

3.2. XRD characterization of the C/C composites

It can be seen from the optical micrograph of the one-dimensional C/C composite after graphitization at 3000 °C as shown in Fig. 2(a) that the unidirectional C/C composite block has a dense structure and flat surface, and the ribbon-shaped fibers on the surface of block are orderly stacked together perpendicular to the hot-pressing direction. Fig. 2(b) shows a textural diagram of a C/C composite block, displaying the possible stack and arrangement direction of ribbon-shaped carbon fibers (approximate to a rectangular shape) along the main surface under the hot-press.

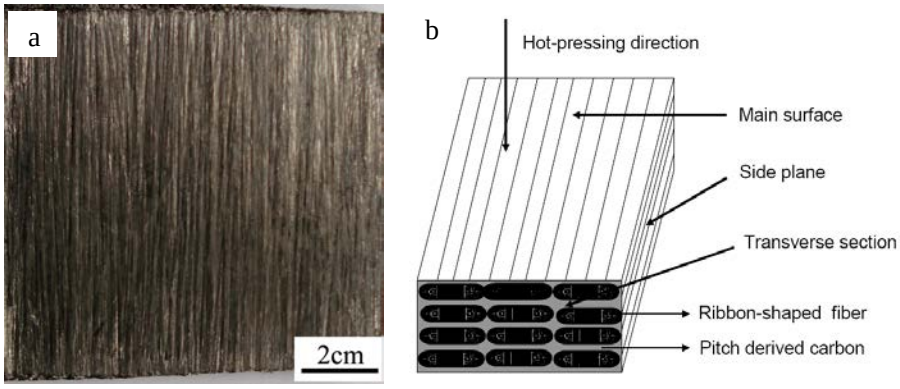

Fig. 2 (a) Optical photograph and (b) textural diagram of one-dimensional C/C composite block.

Fig. 3 shows typical XRD patterns from different planes of the C/C composite product prepared by hot-pressing at 500 °C as well as the product after subsequent treatment at 2800 °C. The XRD profile of the C/C composite block produced by hot-pressing at 500 °C in Fig. 3(a) shows that the crystal orientation of the sample is different. One broad diffraction peak at $2\theta = 25.3°$ from both the main surface and the

side plane of the hot-pressed sample in Fig. 3(a), corresponds to (0 0 2) crystal planes of hexagonal graphite. Two broad diffraction peaks at 2θ = 42.4 and 77.5° from the transverse section of the C/C composite block, corresponding to (1 0 0) and (1 1 0) crystal planes of hexagonal graphite, can be seen in Fig. 3(a). However, the (0 0 2) diffraction peak from the transverse of the C/C composite block disappears. In comparison with the XRD profiles in Fig. 3(a), a sharp (0 0 2) diffraction peak from the main surface and side plane of the graphitized C/C composite can be seen in Fig. 3(b), indicating that the average crystallite size of the graphitized C/C composite obviously increases relative to that of the sample prepared by hot-pressing at 500 °C. No other peaks excluding the strong (0 0 2) and the weak (0 0 4) diffraction peaks are observed due to the highly directional orientation of the carbon layers in the samples [26]. The relative intensity of (0 0 2) diffraction peak of the main surface is obviously stronger than that of the side plane, which results from the more perfect orientation of carbon layers and the larger crystal size of the former as shown in Fig. 1. That is to say that the partial radial or wrinkled crystal texture at the edges of ribbon fibers, as shown in Fig. 1(c and d), decreases the relative intensity of (0 0 2) diffraction peak of the side plane to a certain extent. The (1 0 0) and (1 1 0) diffraction peaks at about 2θ = 42.4 and 77.5° from the transverse of graphitized sample in Fig. 3(b) are obvious stronger and sharper than that of hot-pressed sample. The very strong (0 0 2) diffraction peak from the main surface and side plane of the graphitized C/C composite cannot be observed in the XRD profile of the transverse of the C/C composite in Fig. 3(b). This indicates that after graphitization the crystal coherence length (*L*a, (1 0 0)) and the stacking height (*L*c, (0 0 2)) of the C/C composite increase. The strong (1 0 0) and (1 1 0) diffraction peaks from the transverse of graphitized C/C composite and the strong (0 0 2) diffraction peak from the main surface and side plane

of the graphitized C/C composite suggest that the graphene layers of the graphitized C/C composite are also as highly oriented as its ribbon fibers. It indicates that the highly oriented ribbon-shaped fibers are perfectly aligned in the direction perpendicular to the transverse of composite block [27,28]. The result is well consistent with the textural diagram of a C/C composite block shown in Fig. 2(b), as anticipated above. The resultant one-dimensional C/C composite blocks show an anisotropic nature similar to their ribbon fibers.

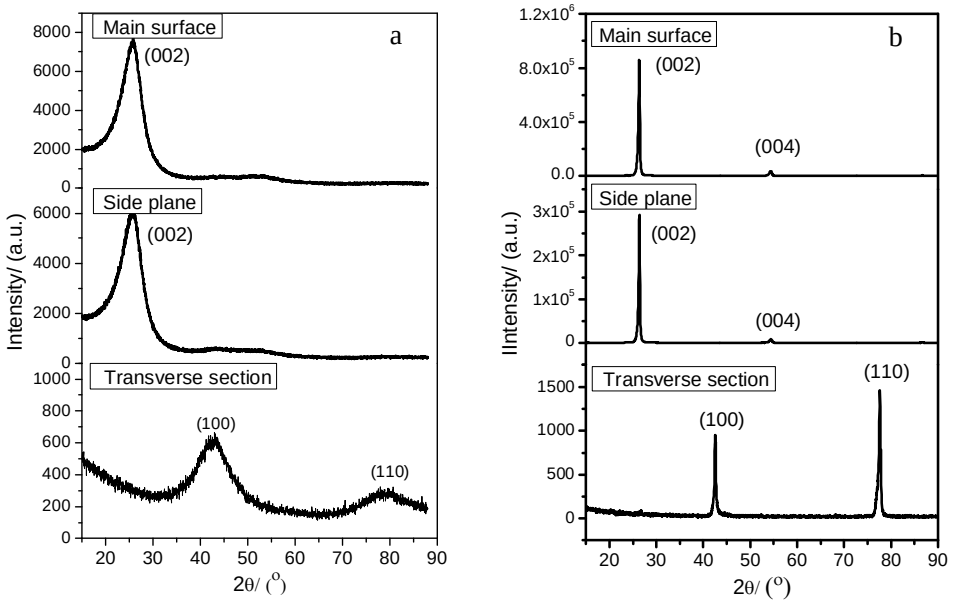

Fig. 3 XRD patterns from different planes of one dimensional C/C composite blocks produced by (a) hot-pressed at 500 °C and (b) subsequently heated at 2800 °C.

Fig. 4(a-c) and Fig. 4(d) show XRD patterns of three orthogonal planes and X-ray powder diffraction patterns of the C/C composite blocks heat treated at different temperatures range from 1000 to 3000 °C. As can be seen from Fig. 4(a-c), the intensities of (0 0 2), (1 0 0) and (1 1 0) diffraction peaks from the different planes of the C/C composite blocks gradually increase with the HTTs and are significantly greater than that of the hot-pressed samples.

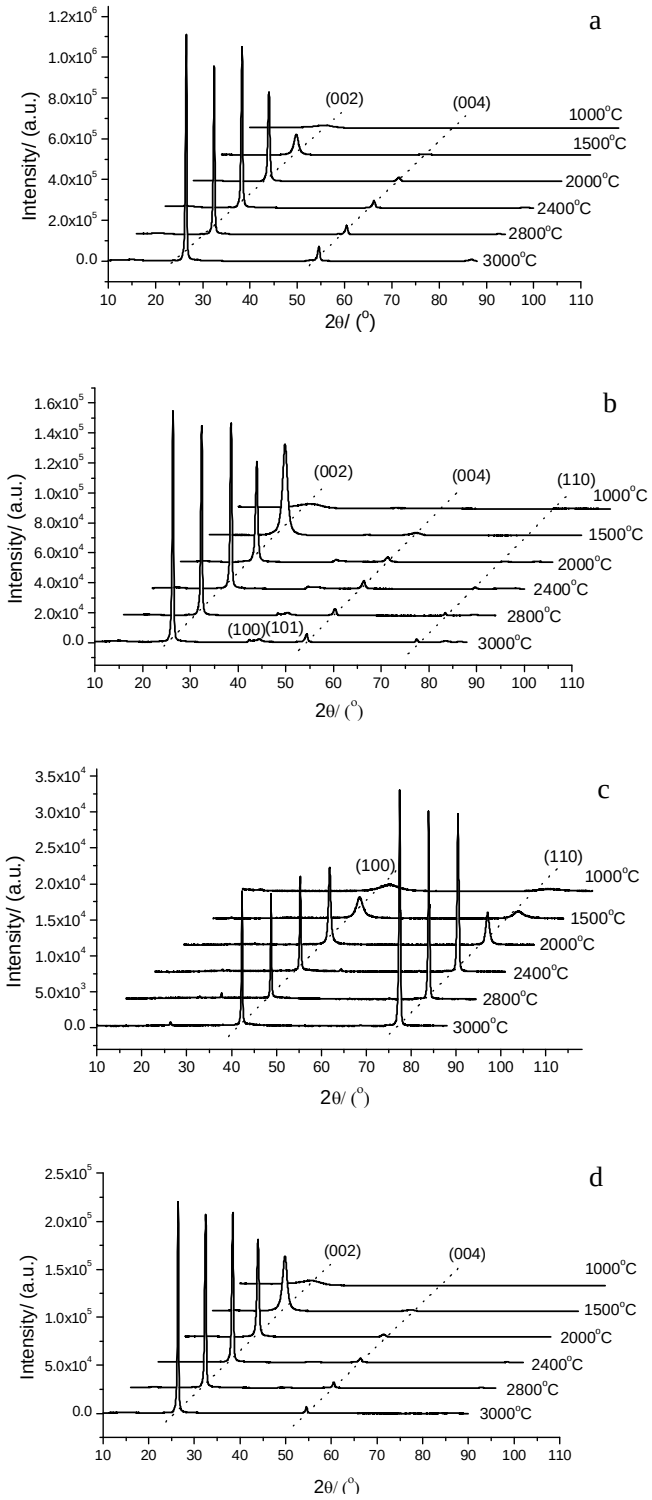

Fig. 4 (a-c) XRD patterns of different planes (a-main surface, b-side plane, c-transverse section) and (d) X-ray powder diffraction patterns of the C/C composite blocks heat treated at different temperatures.

Table 1 Crystalline parameters and degree of graphitization of the C/C composite blocks heat treated at different temperatures.

HTTs/ °C	$2\theta_{002}$/ °	d_{002}/ nm	$Lc_{(002)}$/ nm	$La_{(100)}$/ nm [a]	g/ % [b]
1000	25.36	0.3502	3.74	5.82	—
1500	25.83	0.3440	7.08	8.1	0
2000	25.98	0.3426	18.41	24.80	16.3
2400	26.33	0.3382	27.63	53.56	67.4
2800	26.46	0.3365	36.87	68.20	87.2
3000	26.49	0.3361	44.23	78.30	91.8

[a] $La_{(110)}$ values were calculated according to the (1 0 0) diffraction peak of the transverse section of the C/C composite blocks as shown in Fig. 4(c).

[b] Degree of graphitization (g) was calculated by the expression $g = (0.3440 - d_{002})/(0.3440 - 0.3354)$.

The XRD profiles, from the side plane of the C/C composite blocks after graphitization at 2000~3000 °C in Fig. 4(b), show several weak diffraction peaks corresponding to the (1 0 0), (1 0 1) and (1 1 0) crystal planes of graphite. However, these diffraction peaks cannot be seen in the XRD profiles from the main surface of the C/C composite blocks heat-treated at various temperatures. This can be due to the more perfect orientation of graphene layers at the main plane of the ribbon fibers, along their longitudinal direction and the main surface, than that of the edges of the ribbon fibers as shown in Fig. 1. The X-ray powder diffraction patterns of the C/C composites shown in Fig. 4(d), which are used in the measurement of the interlayer spacing (d_{002}), $La_{(100)}$ and $Lc_{(002)}$, show similar diffraction patterns to that of main surface and side plane of the C/C composites. The intensity of (0 0 2) diffraction peak

is lower and higher than those of the main surface and side plane of the C/C composite blocks shown in Fig. 4(a and b). Being calculated from XRD results, the crystalline parameters and degree of graphitization of the C/C composite blocks are listed in Table 1. The Crystalline parameters ($Lc_{(002)}$ and $La_{(100)}$ values) and degree of graphitization of the C/C composite blocks are remarkably improved with the increase of HTTs.

3.3. SEM and PLM observation of the C/C composites

In order to further understand the anisotropic properties of the C/C composite blocks, the microstructure and morphology of the three orthogonal planes (main surface, side plane and transverse) as well as the optical texture of C/C composite blocks were investigated. Typical SEM images from the main surface and side plane of the C/C composite blocks graphitized at 3000 ℃ are shown in Fig. 5. The parallel stretched and evenly arranged ribbon fibers in the main surface and the side plane of C/C composite block can be observed in SEM images shown in Fig. 5(a and b). Some obvious slits can be seen in the SEM image of the side plane in Fig. 5(b), which results from the interspaces among the stacked ribbon fibers. The high shrinkage of the ribbons perpendicular to the main plane of the ribbon resulting from the structural anisotropy may contribute to the formation of the slits observed. The microstructure differentia of the C/C composite block in the main surface and side plane, may result from the gaps among the ribbon fibers and the incongruent shrinkage rate between the ribbon fibers and mesophase pitch binder. The almost rectangular geometry of the ribbon fibers and the molding pressure lead to the stacking arrangement of the ribbon fibers along the main plane of ribbon fibers to form the highly oriented unidirectional C/C composite block.

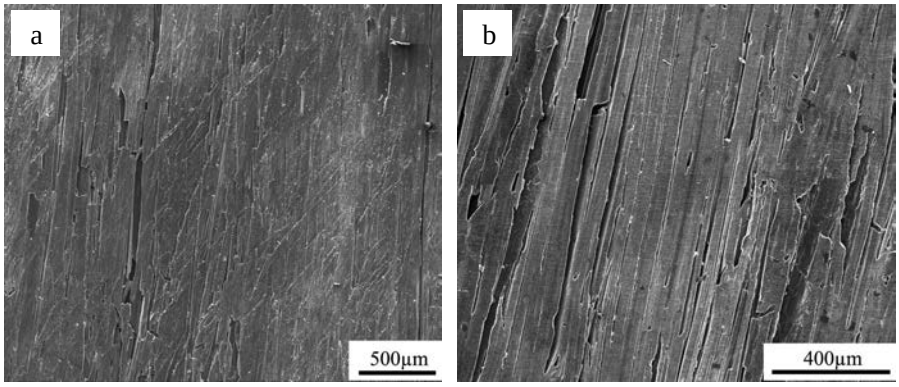

Fig. 5 SEM images of (a) main surface and (b) side plane of the highly oriented C/C composite block graphitized at 3000 °C.

Typical SEM images of the transverse section of the C/C composite block graphitized at 3000 °C are shown in Fig. 6. The low magnification images shown in Fig. 6(a and b) indicate that the composite block possesses a relatively low porosity and a lamellar compacted structure. A layered graphite structure having highly preferred orientation, with the graphite layers mostly stacked parallel to each other, is clearly presented in Fig. 6(c and d) by high magnification observation, showing that the microstructural orientation within the ribbon fibers is still retained. However, the degree of preferred orientation of graphite layers in the transverse section of C/C composite blocks is slightly inferior to that of graphitized ribbon fibers with perfect crystal orientation shown in Fig. 1, which may result from the obvious volume contraction of mesophase pitch binder during carbonization. The preferential contraction of the binder phase relative to the (0 0 2) planes of the ribbon fiber phase, may squeeze the ribbon fibers in the direction of their long transverse axis. Therefore, the growth of graphite crystals has been constrained to some extent. The mesophase pitch derived carbon at the interfaces among the ribbon fibers cannot be clearly identified. It implies that the pitch matrix carbon also has an oriented structure and closely encompasses the highly oriented ribbon fibers, thus resulting in the

disappearance of (0 0 2) diffraction peak from the transverse of graphitized block shown in Fig. 4(c).

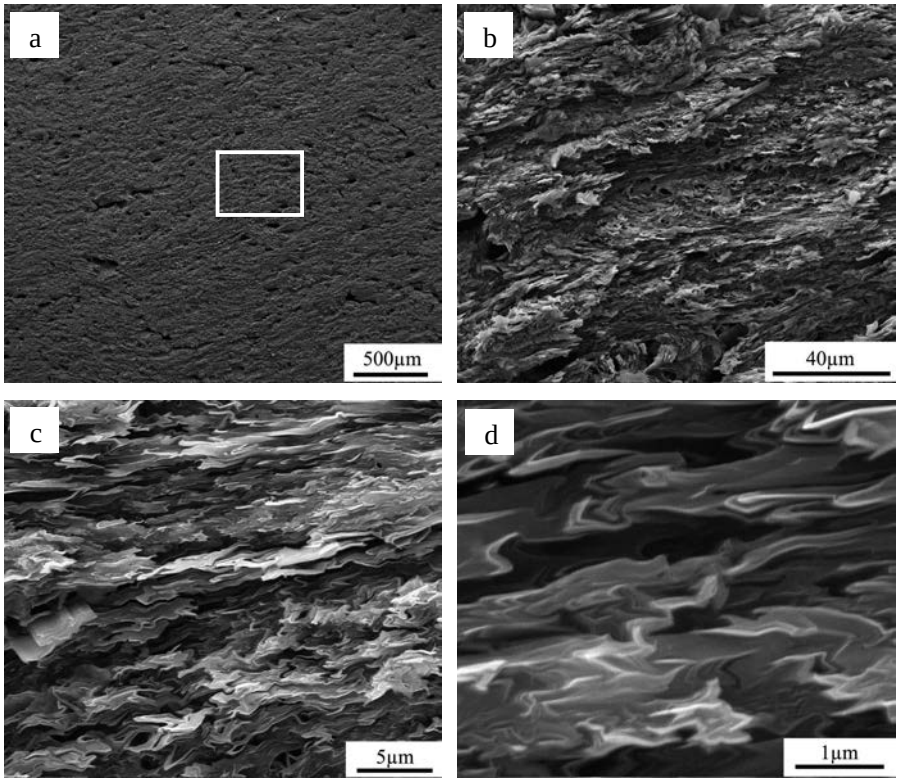

Fig. 6 SEM images of (a-d) transverse section of the highly oriented C/C composite block graphitized at 3000 °C at various magnifications, (b) is the magnified image from the box in (a).

The typical PLM micrographs of the transverse section of the highly oriented C/C composite after graphitization treatment at 3000 °C are shown in Fig. 7 imaged at two orthogonal directions by rotating the object stage of the polarized light microscope. A distinct difference in the interference colors from the images in Fig. 7 can be seen. Ribbon-shaped carbon fibers are stacked parallel to each other and oriented perpendicular to the hot-pressing direction, which corresponds with the textural diagram of a C/C composite block shown in Fig. 2(b). The shape of the ribbon fibers in the transverse section of the C/C composite block is nearly maintained without any

damage in the process of hot-pressing and subsequent heat treatment at high temperatures. The mesophase pitch binder carbon seems to be uniformly distributed among ribbon-shaped carbon fibers and to form a partially oriented structure around the ribbon fibers. During hot pressing, the mesophase pitch binder softened, deformed and tended to preferentially orient along the main plane of the ribbon fibers. There is no obvious debond or crack occurring at the interface between the ribbon fiber and its matrix. The low porosity, highly oriented graphite layers and complete ribbon shape of fibers can be expected to aid transport phenomena, thus leading to higher electrical and thermal conductivity of unidirectional C/C composite along the longitudinal direction of ribbon fibers, as will be shown subsequently.

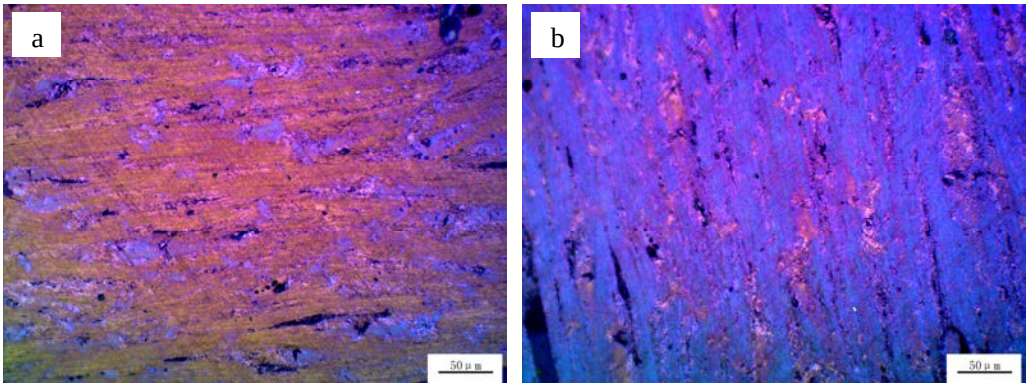

Fig. 7 Typical PLM micrographs of transverse section of the highly oriented C/C composite block graphitized at 3000 °C showing the orientation of ribbon-shaped carbon fibers viewed in two different orthogonal directions (a) and (b).

3.4. Electrical and thermal properties of the C/C composites

The bulk densities, electrical resistivities and thermal conductivities (i.e. along the longitudinal direction of ribbon fibers) of the C/C composites heat treated at different temperatures (500 to 3000°C) are shown in Fig. 8. As can be clearly seen from the plots shown in Fig. 8(a) that the bulk densities and electrical resistivities of the C/C

composites generally increase and decrease with the increase of HTTs. The bulk density of the hot-pressed C/C composites is only about 1.32 g/cm^3, slightly higher than that of mesophase pitch (1.25 g/cm^3), whereas the bulk density of the C/C composite samples graphitized at 2000 °C reaches a maximum value of 1.88 g/cm^3 as a result of macroscopic volume shrinkage above 30%, without any densification by impregnation or chemical vapor deposition treatments, which are known to be time-consuming, complicated and expensive. As the HTT reaches to 3000 °C, the bulk density of C/C composites slightly decreases to 1.86 g/cm^3, which may be related to the different growth rates of the graphite crystals in the different crystal preferred orientations at the edges and center of ribbon fibers.

The electrical resistivity of the hot-pressed C/C composites at 500 °C is about 29.6 Ω m, which is similar to that of a pitch derived semicoke heat treated at 550 °C [29]. As the HTT reaches to 1000 °C, the electrical resistivity of the C/C composites significantly decreases to 14.6 μΩ m. At this stage the continuous carbon phase has been formed in the composite block since the ribbon fibers and mesophase pitch binder were both completely pyrolysed or carbonized during the carbonization. The creation of mobile π electrons [30] thus leads to the rapid decrease in electrical resistivity of the C/C composites. Upon further heat treatment of the C/C composites up to 2000 °C, the electrical resistivity of the samples continuously decreases further to 3.4 μΩ m and when graphitized at 3000 °C, the electrical resistivity is as low as 1.6 μΩ m, which (within experimental limitations and errors) is close to that for a single graphite flake in the in-plane direction, which lies in the range of 0.5~1.0 μΩ m [31]. The electrical resisitivies of the C/C composites graphitized at 3000 °C along another two directions (i.e., perpendicular to the side plane and main surface of C/C composite blocks) are 1.7 and 22.2 μΩ m. The high value of electrical resistivity in

the direction perpendicular to the main surface of C/C composite block is associated to the lamellar structure comprising a multi-layered stack of ribbon fibers, and the lower electrical conductivity in the crystal ‘c’ direction.

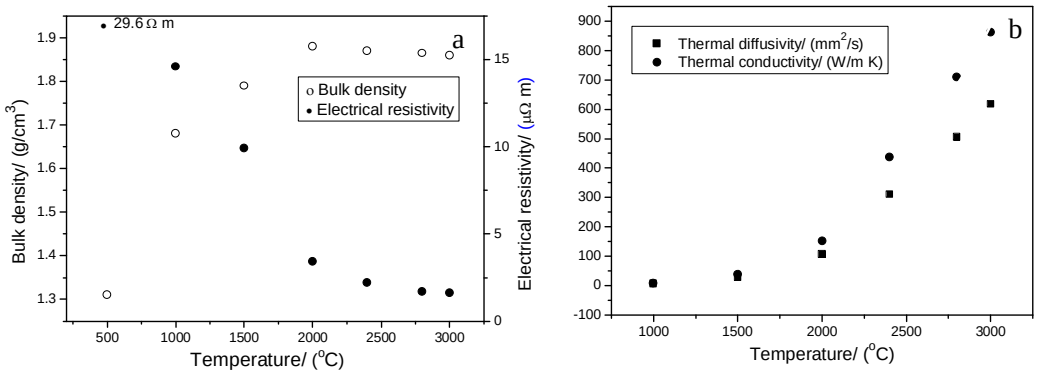

Fig. 8 (a) Bulk densities - electrical resistivities and (b) thermal diffusivity - thermal conductivities of the C/C composites as a function of HTTs.

Fig. 8(b) shows that the thermal diffusivity and thermal conductivity of C/C composites along the longitudinal direction of ribbon fibers both markedly increase with the HTTs. For the C/C composites carbonized below 1500 °C, the thermal diffusivities and thermal conductivities at room temperature are as low as 28 mm^2/s and 38 W/m K, respectively. After graphitization, the thermal transport properties of C/C composites are markedly improved. In the case of C/C composites graphitized at 3000 °C, the thermal diffusivity and thermal conductivity values increase significantly to be as high as 618 mm^2/s and 862 W/m K, respectively. This is because during heat treatment to 3000 °C, the highly oriented mesophase pitch-based ribbon fibers and mesophase pitch binder become strongly graphitized [32,33]. With the increase of HTTs, the graphite crystallites become larger and more perfect as discussed in Fig. 4 as well as have a more entire lamellar stacking structure and better orientation as shown in Fig. 6 and Fig. 7, and this significantly increases the thermal conductivity.

With further increase the graphitization temperature to 3100 °C, the thermal diffusivity and thermal conductivity values of C/C composite, along the longitudinal direction of ribbon fibers, increase to 642 mm^2/s and 896 W/m K, respectively. These values are much higher than those of reported in the former recited literatures [7,10-13] and traditional metal materials used for thermal management [34], in addition, the corresponding values for copper are only 117 mm^2/s and 398 W/m K. The bulk density of the graphitized C/C composite blocks is about 1.86 g/cm^3, less than a quarter of that of copper (8.9 g/cm^3). This means that the specific thermal conductivity of the C/C composite block is ten times higher than that of copper. However, the corresponding electrical resistivities of the C/C composite samples graphitized at 3100 °C nearly have no change (from 1.6 to 1.5 μΩ m), which means that the HHT plays an important role in improving the thermal transport property of the C/C composites.

For the C/C composite blocks graphitized at 3000 °C, the thermal diffusivity and thermal conductivity values measured in the direction perpendicular to the side plane of the C/C composite block dramatically decrease to 41 mm^2/s and 57 W/m K, which means that the entire crystal orientation of graphite and the quantity of crystal interfaces in the blocks (resulting from the difference in the crystal structure and orientation of the ribbon fiber as shown in Fig. 1), play important roles in improving the thermal transport property of the C/C composites, although the electrical resistivity along this direction has no obvious change (varying between 1.6 and 1.7 μΩ m). The corresponding thermal diffusivity and thermal conductivity values measured in the direction perpendicular to the main surface of the C/C composite block are measured to be as low as 8 mm^2/s and 11 W/m K. This thermal conductivity value is very close to the theoretical limit value of 6~10 W/m K for crystalline

graphite perpendicular to the basal plane [35]. The very high anisotropy ratio of ~80:1 for the thermal conductivity in the two principal directions (i.e., perpendicular to the transverse and main surface of C/C composite blocks) reflects the higher degree of preferred orientation of the graphite layers in the longitudinal direction of ribbon fibers. The resultant one-dimensional C/C composite blocks exhibit a typical three-dimensional anisotropic thermal conductive behavior, which is consistent with the result reported by Ma's group [13]. In comparison, Ma et al. [12,13] have reported that the thermal conductivity of graphite materials (along the direction parallel to the fiber axis) made with narrow ribbon fibers with an average cross section of 27 × 6 μm was about 837 W/m K, while the calculated thermal diffusivity value was about 540 mm^2/s (if the C_p is defined as 0.71 J/g K). The higher thermal diffusivity (above 618 mm^2/s) of the former may result from the better crystal orientation and larger crystallite sizes in the composite blocks.

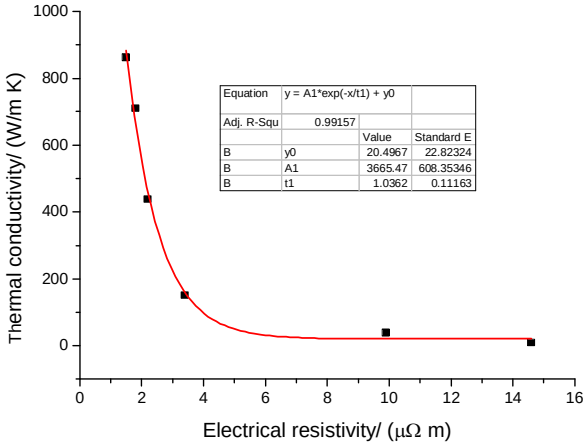

Fig. 9 Correlation between thermal conductivities of the C/C composites along the longitudinal direction of ribbon fibers versus their electrical resistivities.

There exist good empirical correlations between the measured axial electrical conductivity and the thermal conductivity for mesophase pitch-based carbon fibers

with round [36-38] and ribbon [36] shaped sections along the direction of fiber axis, since the electrical and thermal conductive properties vary with structure in the same way. According to the above mentioned empirical correlations, the calculated axial thermal conductivity of 3000 °C graphitized ribbon fibers, based on 1.08 μΩ m of axial electrical resistivity of the fibers, ranges from 907 to 1167 W/m K, which is comparable to or even superior to that of K-1100 graphite fiber (the axial electrical resistivity of K-1100 graphite fiber is about 1.17 μΩ m when measured in the same way and its calculated thermal conductivity varies from 878 to 1077 W/m K). This result is agreement with the thermal conductivity value of similar ribbon-shaped fibers, about 1000 W/m K, reported by Rand et al [18]. Considering that the geometry limits the volume fraction of fiber in the composite, the measured thermal conductivity of the ultimately graphitized one-dimensional C/C composite must be inferior to that of graphitized ribbon fibers [18] and K-1100 graphite fibers [6]. However, the thermal conductivity of the present C/C composites can be compared to that value (about 900 W/m K) of narrow ribbon-shaped fibers with a width of 20~30 μm reported in reference [16]. In addition, the thermal conductivity of the ribbon fibers (calculated by the corresponding electrical resistivity) has been brought into play at least 80% in the highly oriented one-dimensional C/C composite. In the case of the prepared one-dimensional C/C composites, which mainly comprise unidirectional arranged ribbon fibers with a volume content of about 90% determined through the observation of PLM, may also have a similar correlation of thermal conductivity and electrical resistivity along the longitudinal direction of ribbon fibers, which is clearly shown in Fig. 9. As can be seen from the graph in Fig. 9, there is a reasonably good fit with a high correlation coefficient of 0.99 for the thermal conductivity and electrical resistivity of the resulting C/C composites. Such a high correlation coefficient is

associated with the highly oriented structure and continuous structural integrity in the longitudinal direction of ribbon fibers. Though the carriers involved in both transport phenomena, phonons for the thermal conductivity and electrons and/or holes for the electrical resistivity are different, the correlation between thermal conductivity and electrical conductivity in a specific direction is quite good. So, for one-dimensional C/C composites derived from the same mesophase pitch precursor, once the electrical resistivity is known, the corresponding thermal conductivity may be approximately estimated.

It is now well accepted that the thermal conductivity of single crystal and polycrystalline forms of graphite at temperatures in the range of 200 to 1000 K is dominated by phonons (lattice vibrations). Thermal transport by phonons is limited by two principal mechanisms: scattering at crystallite grain boundaries, and scattering at point defects within the layer planes. The first is associated with the planar crystallite size; the second is less straight forward to assess [11]. Fig. 10 shows plots of the thermal conductivity of the highly oriented C/C composites along the longitudinal direction of ribbon fibers versus their microcrystal parameters d_{002}, Lc and La. The Lc and La values were calculated by a powder XRD measurement through a line-broadening analysis using the Scherrer equation. As a comparison, the La values were also calculated by the relationship based on the d_{002} value reported in references [39,40] because of no obvious (1 0 0) and (1 1 0) diffraction peaks appeared in the X-ray powder diffraction patterns as shown in Fig. 4(d) for such highly oriented carbon materials. From the Fig. 10(a), it can be seen that there exists exponential correlation between the thermal conductivities versus d_{002}, which is related to the big interval of HTTs range from 1000 to 3000 ℃, and the corresponding intrinsic structure of the C/C composite blocks undergoes from essentially turbostratic

(unordered carbon) to perfectly graphitic structure. However, the thermal conductivities linearly correlate with *L*c and *L*a as shown in Fig. 10(b and c), which is consistent with the results have been reported in the past references [41,42].

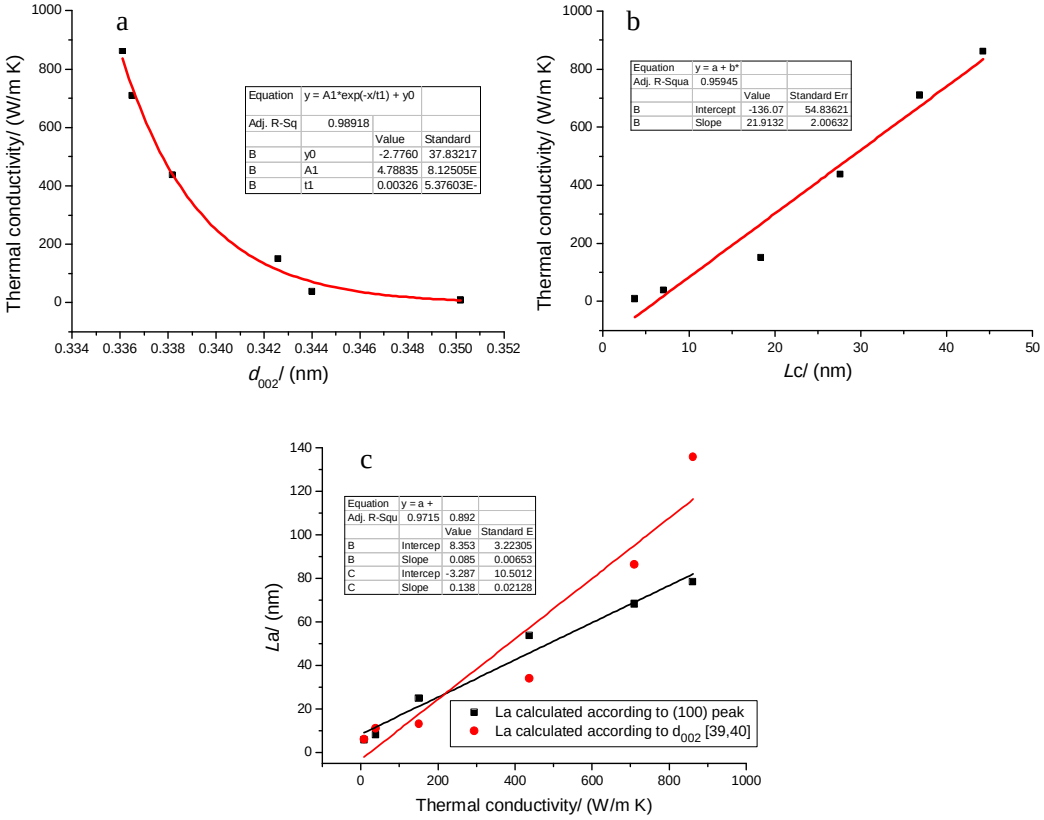

Fig. 10 Correlation between thermal conductivities of the C/C composites along the longitudinal direction of ribbon fibers versus their microcrystal parameters (a) d_{002}, (b) *L*c and (c) *L*a.

The correlation coefficients for the thermal conductivities and *L*a values (calculated by different methods) shown in Fig. 10(c) are 0.97 and 0.89, which seems to indicate it is more feasible to calculate *L*a values according to the (1 0 0) diffraction peak of such highly oriented materials. In addition, the correlation coefficients (shown to two decimal places) for the thermal conductivities versus d_{002}, *L*c and *L*a are as high as 0.99, 0.96 and 0.97 for Fig. 10(a-c), respectively, which are much higher than those

(0.8, 0.7 and 0.4) previously reported [11]. The reason is that the structure and orientation of the resulting C/C composite blocks are better than those of the Thermal Graph panels [11]. The good linearly correlation between the thermal conductivities and *L*a means that the thermal transport mechanism in such high oriented C/C composites is closely associated with the planar crystallite size of *L*a, i.e., the phonon mean free path, and the preferred orientation and structural continuity of graphite crystals or layers in the blocks mostly dominate the thermal conduction.

3.5. Mechanical properties of the C/C composites

The bending strengths in the two principal directions (i.e., perpendicular to the main surface and side plane of C/C composite blocks) for the C/C composite blocks graphitization treated at 3000 °C are measured to be 35.2 MPa and 56.8 MPa, respectively. The obviously mechanical difference in the two directions results from the structural differentia as shown in Fig. 5. This is due to the lamellar structure consisting of the ribbon fiber' main planes stacked on the main surface of the C/C block, which makes it easier for the ribbon fibers to slide past each other and induce delaminating behavior under bending stress in this direction, compared to the direction along side plane of the C/C composite block. The weak binding forces/ adhesion between ribbon fibers with smooth fiber surfaces and graphite derived from the mesophase pitch binder, along with the brittle fracture behavior of the graphitic ribbon fibers, means that the bending strength of the C/C composite blocks is not high. The relatively low bending strength in comparison with earlier work reported by Ma et al. [12,13] is due to the higher crystal orientation of ribbon fibers and their C/C composites as well as larger transverse area of the ribbon fibers. How to improve the mechanical properties of such highly oriented materials is still under study.

4. Conclusions

Highly oriented one-dimensional C/C composites with a relatively high bulk density of 1.86 g/cm^3 were fabricated by a simple hot-pressing (~500 °C) method combined with subsequent carbonization and graphitization treatments. The parallel stretched and unidirectional arranged ribbon fibers are evenly stacked along the hot-pressing direction in the graphitized one-dimensional C/C composites. XRD shows that the graphite crystallites within the ribbon fibers are also well aligned with their crystalline a-directions parallel to both the main surfaces of the C/C composite blocks and the longitudinal direction of ribbon fibers. The prepared C/C composite blocks possess a typical three-dimensional structural anisotropy, which results from the anisotropic structure of the ribbon fibers themselves and the unidirectional arrangement of the ribbon fibers in the C/C composite, and thus leads to the obvious differentia in the electrical and thermal conductive behaviors of the C/C composite along three orthogonal planes. Both the electrical resistivity and thermal conductivity are both found to be dominated by HTT, and markedly decrease and increase with the increasing of HTTs. After graphitization at 3000 °C, the C/C composite blocks possess a low electrical resistivity of 1.6 μΩ m and a ultrahigh thermal conductivity of 862 W/m K with a correspondingly high thermal diffusivity of 618 mm^2/s along the longitudinal direction of ribbon fibers at room temperature, which further increase to 642 mm^2/s and 896 W/m K as the HTT rises up to 3100 °C, although the electrical resistivity (1.5 μΩ m) has no obvious change. The electrical resistivities and thermal conductivities perpendicular to the side plane and main surface of C/C composite blocks graphitized at 3000 °C are 1.7 and 22.2 μΩ m, 57 and 11 W/m K, respectively. The room-temperature thermal conductivities of the highly oriented C/C composite blocks (along the longitudinal direction of ribbon fibers) have close relationships with

the corresponding electrical resistivities and graphitic microcrystallite parameters (d_{002}, Lc, La). The correlation coefficients are all as high as above 0.9. Despite the relatively low bending strengths of the C/C composite blocks, which are generally consistent with their highly anisotropic structure, their thermal conductivities in the longitudinal direction of ribbon fibers are significantly higher than that of copper. Hence these oriented C/C composite materials with a low weight (compared to metals) have strong potential application as heat-sinks/ heat spreaders in advanced thermal management to replace other more traditional heat conducting materials.

Acknowledgements

This work was sponsored by the Key Program of Major Research Plan of the National Natural Science Foundation (grant No. 91016003) and the National Natural Science Foundation (grant No. 51372177) of China. The authors sincerely thank Dr. Shaoxin Zhou for thermal conductivity measurements.

References

[1] Fitzer E. The future of carbon-carbon composites. Carbon 1987;25(2):163−90.

[2] Sheehan JE, Buesking KW, Sullivan BJ. Carbon-carbon composites. Annu Rev Mater Sci 1994;24:19−44.

[3] Lackey WJ. Carbon-carbon composites. In: Buschow KHJ, Cahn RW, Flemings MC, Iischner B, Kramer EJ, Mahajan S, Veyssiere P, editors. Encyclopedia of materials: science and technology. London: Pergamon Pr Publisher; 2001, P. 952−67.

[4] Manocha LM. Thermophysical properties of densified pitch based carbon/carbon materials-I. Unidirectional composites. Carbon 2006;44(3):480−7.

[5] Singer LS. Carbon fibers from mesophase pitch. Fuel 1981;60(9):839−47.

[6] Minus ML, Kumar S. The processing, properties, and structure of carbon fibers. JOM 2005;57(2):52−8.

[7] Kude Y, Sohda Y. Thermal management of carbon-carbon composites by functionally graded fiber arrangement technique. In: Shiota I, Yiyamoto, editors. Functionally graded materials. Oxford: Elsevier Science Imprint; 1996, P. 239−44.

[8] Edie DD. The effect of processing on the structure and properties of carbon fibers. Carbon 1998;36(4):345−362.

[9] Zweben C. High-performance thermal management materials. Adv Packaging 2006;15(2):1−5.

[10] Bowers DA, Davis JW, Dinwiddie RB. Development of 1-D carbon composites for plasma-facing components. J Nucl Mater 1994;212-215:1163−7.

[11] Adams PM, Katzman HA, Rellick GS, Stupian GW. Characterization of high thermal conductivity carbon fibers and a self-reinforced graphite panel. Carbon 1998;36(3):233–45.

[12] Ma ZK, Shi JL, Song Y, Guo QG, Zhai GT, Liu L. Carbon with high thermal conductivity, prepared from ribbon-shaped mesophase pitch-based fibers. Carbon 2006;44(7):1298–352.

[13] Ma ZK, Liu L, Lian F, Song HH, Liu J. Three-dimensional thermal conductive behavior of graphite materials sintered from ribbon mesophase pitch-based fibers. Mater Lett 2012;66(1):99-101.

[14] Edie DD, Fain CC, Robinson KE, Harper AM, Rogers DK. Ribbon-shape carbon fibers for thermal management. Carbon 1993;31(6):941−9.

[15] Edie DD, Robinson KE, Fleurot O, Jones SP, Fain CC. High thermal conductivity ribbon fibers from naphthalene-based mesophase. Carbon 1994;32(6):1045−54.

[16] Gallego NC, Edie DD, Nysten B, Issi JP, Treleaven JW, Deshpande GV. The thermal conductivity of ribbon-shaped carbon fibers. Carbon 2000;38(7):1003−10.

[17] Lu SL, Blanco C, Appleyard S, Hammond C, Rand B. Texture studies of carbon and graphite tapes by XRD texture goniometry. J Mater Sci 2002;37(24):5283−90.

[18] Rand B, Lu SL, Blanco C, Daniels H, Brydson RMD. Structure and properties of highly oriented mesophase graphite tapes of high conductivity. Extended abstracts, an International Conference on Carbon 2002. Beijing (China): Chinese Carbon Society, 2002; P. 1−4.

[19] Galanopoulos E, Rand B, Westwood A. Wide, highly oriented mesophase pitch-based carbon tapes and their laminates. Extended abstracts, an International Conference on Carbon 2003. Oviedo (Spain): Spanish Carbon Society, 2003; P. 1−4.

[20] Picard S, Burns DT, Roger P. Determination of the specific heat capacity of a graphite sample using absolute and differential methods. Metrologia 2007;44(5):294−302.

[21] Hummel RE. Understanding materials science: history, properties, application. 2nd ed. New York: Springer. 2004: 273.

[22] Yuan GM, L XK, Zhou J, Dong ZJ, Cui ZW, Cong Y, et al. Controlled preparation of mesophase pitch-based highly oriented carbon fibers with different shapes. Extended abstracts, an International Conference on Carbon 2012. Krakow (Poland): Polish Carbon Society, 2012; P. 1−4.

[23] Mochida I, Yoon SH, Takano N, Fortin F, Korai Y, Yokogawa K. Microstructure of mesophase pitch-based carbon fiber and its control. Carbon 1996;34(8):941−56.

[24] Lu SL, Blanco C, Rand B. Large diameter carbon fibres from mesophase pitch. Carbon 2002;40(12):2109−16.

[25] Shinohara K, Fujimoto H. The microstructure of highly-oriented graphite tape

prepared from mesophase pitch by melt-blowing. Carbon 2012;50(13):4926−31.

[26] Yuan GM, Li XK, Dong ZJ, Westwood A, Cui ZW, Cong Y, et al. Graphite blocks with preferred orientation and high thermal conductivity. Carbon 2012;50(1):175−82.

[27] Hishiyama Y, Nakamura M. X-ray diffraction in oriented carbon films with turbostratic structure. Carbon 1995;33(10):1399−403.

[28] Chen GH, Wang HQ, Zhao WF. Fabrication of highly ordered polymer/graphite flake composite with eminent anisotropic electrical property. Poly Adv Technol 2008;19(8):1113−7.

[29] Elalaoui M, Krebs V, Mareche JF, Furdin G, Bertau R. Carbonization of coal-tar pitch under controlled atmosphere-Part II: Effect of temperature and pressure on the electrical property evolution of the formed green coke. Carbon 1995;33(5):653−6.

[30] Dumont M, Dourges MA, Bourrat X, Pailler R, Naslain R, Babot O, et al. Carbonization behaviour of modified synthetic mesophase pitches. Carbon 2005;43(11):2277−84.

[31] Dutta AK. Electrical conductivity of single crystals of graphite. Phys Rev 1953;90(2):187−92.

[32] Brooks JD, Taylor GH. The formation of graphitizing carbons from the liquid phase. Carbon 1965;3(2):185−93.

[33] Horr NE, Bourgerette C, Oberlin A. Mesophase powders (carbonization and graphitization). Carbon 1994;32(6):1035−44.

[34] Chung DDL. Materials for thermal conduction. Appl Therm Eng 2001;21(16): 1593−605.

[35] Norley J. The role of natural graphite in electronics cooling. Electronics Cooling 2001;7:50−1.

[36] Lavin JG, Boyington DR, Lahijani J, Nysten B, Issi JP. The correlation of thermal conductivity with electrical resistivity in mesophase pitch-based carbon fiber. Carbon 1993;31(6):1001−2.

[37] Zhang X, Fujiwara S, Fujii M. Measurement of thermal conductivity and electrical resistivity of a single carbon fiber. Int J Thermophys 2000;21(4):965−80.

[38] Hiroshi H, Masumi H, Tetsuo B. Carbon fiber composite sheet, use thereof as a heat conductor and pitch-based carbon fiber web sheet for use in the same. US patent 20090061193, 2009.

[39] Takahashi H, Kuroda H, Akamatu H. Correlation between stacking order and crystallite dimensions in carbons. Carbon 1965;2(4):432−3.

[40] Kelly BT. Physics of graphite. London: Butterworth. 1981: 21-23.

[41] Kelly BT. Theory of the effect of crystallite boundaries on the principal thermal conductivities of highly oriented graphite. Carbon 1968;6(1):71−80.

[42] Kelly BT. Theory of the effect of crystallite boundaries on the principal thermal conductivities of highly oriented graphite- The effect of the elastic constant C_{44}. Carbon 1968;6(4):485−96.